
RELCHANET: NEURAL NETWORK FEATURE SELECTION USING RELATIVE CHANGE SCORES

Felix Zimmer

Independent Researcher

felix.zimmer@mail.de

ABSTRACT

There is an ongoing effort to develop feature selection algorithms to improve interpretability, reduce computational resources, and minimize overfitting in predictive models. Neural networks stand out as architectures on which to build feature selection methods, and recently, neuron pruning and regrowth have emerged from the sparse neural network literature as promising new tools. We introduce RelChaNet, a novel and lightweight feature selection algorithm that uses neuron pruning and regrowth in the input layer of a dense neural network. For neuron pruning, a gradient sum metric measures the relative change induced in a network after a feature enters, while neurons are randomly regrown. We also propose an extension that adapts the size of the input layer at runtime. Extensive experiments on nine different datasets show that our approach generally outperforms the current state-of-the-art methods, and in particular improves the average accuracy by 2% on the MNIST dataset. Our code is available at <https://github.com/flxzimmer/relchanet>.

1 INTRODUCTION

Feature selection is an elemental task in predictive modelling. It can serve to reduce computational resources, improve interpretability by highlighting important features, or improve predictive performance by reducing overfitting (Li et al., 2018). To further these goals has been the driving motivation of large recent efforts to improve existing and develop new feature selection algorithms. Feature selection algorithms can be categorized into embedded, wrapper, and filter approaches. Embedded methods select features during training of a predictive model, such as linear regression (Tibshirani, 1996) or neural networks (Lemhadri et al., 2021). Wrapper approaches also work around a specific predictive model, but treat it as a black box with the feature set as a hyperparameter, e.g., via particle swarm optimization (Rostami et al., 2021). Filter approaches select feature sets without being tailored around a predictive model, but using information-theoretic measures. They include, for example, statistical tests of the relationship between the feature and the outcome (Bommert et al., 2020).

Neural networks have a great ability to capture nonlinear relationships and offer many entry points for slightly modifying their architecture or training algorithm to build successful embedded feature selection methods. To decide on the utility of an input neuron, approaches added gates in the input layer (Yamada et al., 2020), added residual connections to the output (Lemhadri et al., 2021), or added gradients with respect to data changes to the loss (Cherepanova et al., 2023).

Feature selection in neural networks translates to aiming for a sparse input layer and is therefore a special case of sparse neural networks (Hoefler et al., 2021). Recently, it was shown that sparse neural network training, which employs neuron pruning and regrowth (Mocanu et al., 2018; Evci et al., 2020), can be adapted to achieve a dominant feature selection performance (Liu et al., 2024; Atashgahi et al., 2024; Sokar et al., 2024). However, we have identified potential improvements to enhance the network’s ability to detect important features and make it easier for regrown neurons to compete with established neurons during training.

In this paper, we introduce RelChaNet, a novel neural **network** feature selection algorithm using **relative change scores**. It applies neuron pruning and regrowth in the input layer of a dense neural network based on a relative change metric shown in Figure 1. Our main contributions are:

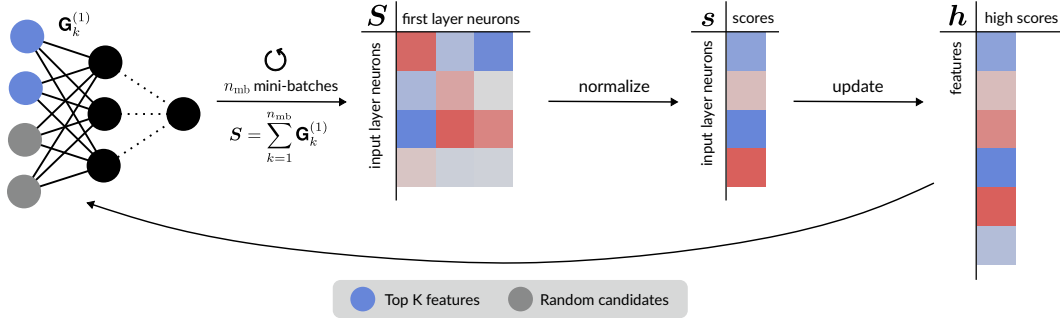


Figure 1: Illustration of the relative change score calculation embedded in RelChaNet, Algorithm 1. We consider a neural network with an input layer size equal to the number of features to select, K , plus additional candidate features. Over several mini-batches, determined by the hyperparameter n_{mb} , the first layer gradients $\mathbf{G}_k^{(1)}$ are accumulated in a matrix \mathbf{S} . Next, these gradient sums are normalized by taking the L^1 norm with respect to each input neuron, followed by z-standardizing the resulting vector to produce a score vector \mathbf{s} . The scores of all candidates are then used to update the high scores \mathbf{h} . Finally, features among the top K high scores remain in the network, while the other features are randomly redrawn. Before continuing training, the first layer weights of candidate features are reinitialized.

1. The RelChaNet feature selection algorithm, which has two key hyperparameters that allow it to adapt to the characteristics of the dataset used. It addresses two identified drawbacks by giving candidates multiple mini-batches of time to show their potential relevance in the network, and by comparing relevance as determined by the change induced rather than by absolute weights.
2. A version of the algorithm that can adapt the input layer size during runtime, making the algorithm less sensitive to one of its hyperparameters.
3. An evaluation of the approach on nine diverse datasets, demonstrating that it generally outperforms the current state-of-the-art.

The structure of this paper is as follows: We begin with a review of related work, particularly focusing on neural network-based methods. Next, we present the RelChaNet algorithm and its extension with an adaptive input layer size. We then conduct an extensive experiment to empirically evaluate our approach. Finally, we perform auxiliary analyses to investigate its design parameters and computational efficiency.

2 BACKGROUND AND RELATED WORK

In this section, we introduce the feature selection problem in a neural network formulation and review previous solution approaches. Most approaches slightly modify a dense neural network architecture or the loss function. Recently, successful approaches have been taken from the framework of sparse neural networks.

Feature selection in neural networks. We consider the task of selecting a set of K features that are most valuable for making accurate predictions in a supervised learning setting. Specifically for neural networks, we can express this task using L^0 regularization of the first layer network weights. Accordingly, we want to optimize the network under the condition that only K input neurons are active, i.e., have any non-zero adjacent weights. If we consider a neural network with one input neuron for each feature $i \in \{1, \dots, N\}$, $N > K$, we can express the feature selection task as finding a specific set of network weights \mathbf{W} that fulfills

$$\arg \min_{\mathbf{W}} \left\{ \mathcal{L}(\mathbf{W}) \mid \#\{i \mid \|\mathbf{W}_i^{(1)}\|_1 > 0\} = K \right\} \quad (1)$$

where $\mathcal{L}(\mathbf{W})$ represents evaluating the loss function \mathcal{L} using the data and network weights, and $\mathbf{W}_i^{(1)}$ is the vector of outgoing first layer weights from input neuron i .

Dense neural networks. There are several methods embedded in dense neural networks for feature selection. A common property is that the number of active neurons is not strictly enforced before model convergence. Instead, selection is gradual, starting with a full input layer of N neurons and reducing active neurons during training. This approach makes it easier to identify complex interactions between features, at the cost of increased computational complexity. Stochastic gates (Yamada et al., 2020) approach the L^0 regularization by adding a gate to each input layer neuron. For each gate, a trainable parameter controls the probability of a feature being active. The LassoNet (Lemhadri et al., 2021) adds a residual connection from each input layer neuron to the network output. The absolute sizes of these N residual weights are added to the loss function and for each feature i individually represent a bound on the size of the corresponding first layer weights, $\|\mathbf{W}_i^{(1)}\|_1$. A less invasive approach is DeepLasso (Cherepanova et al., 2023), which adds the gradient with respect to changes in the input data to the loss function. This encourages the network not to use some features during training, rendering the corresponding input neuron inactive.

Sparse neural networks. Sparse neural networks keep a large fraction of the weights throughout the network at 0 to reduce memory requirements or training time (Hoeffler et al., 2021). One method to achieve this is to prune neurons, i.e., set all of a neuron’s outgoing weights to 0. Metrics for deciding which neurons to prune include the magnitude of outgoing weights or the sensitivity of the output to the neuron. Training sparse neural networks can also involve neuron regrowth, where neurons are periodically added based on criteria such as the size of gradients of adjacent weights. Molchanov et al. (2019) propose a pruning method that calculates a score across mini-batches, similar to our approach. However, their method is not specific to the input layer, calculates the product of weight and gradient, and does not involve regrowing neurons or reusing a score later in training. GradEnFS (Liu et al., 2024) leverages the framework of sparse neural networks for feature selection and, similar to DeepLasso, measures neuron importance using the loss sensitivity to changes in the input neurons. After convergence, the algorithm selects features with the top K neuron importance, which we see as a disadvantage as no specific sets of K features are assessed during training.

Since pruning the input layer reduces the number of active neurons, as required in Equation 1, methods that do so are promising for feature selection. NeuroFS (Atashgahi et al., 2023) does this by extending adaptive sparse neural network training to the input layer (Mocanu et al., 2018; Evci et al., 2020). An input neuron i can be pruned after each epoch based on the size of its outgoing connections, $\|\mathbf{W}_i^{(1)}\|_1$. To regrow an input neuron, the approach calculates the absolute gradients of all currently pruned first layer connections and adds those neurons that have at least one gradient among the highest absolute gradients. During training, the number of active neurons in the input layer is continuously reduced. After training, the input neurons with the largest outgoing connections among the remaining active neurons are selected.

We generally observe two drawbacks in gradient-based regrowing and absolute weight-based pruning for feature selection. Firstly, in the regrowing procedure, features need to signal their importance through high gradients before the network makes any adjustments for them. However, the network might take longer, e.g., multiple mini-batches, to recognize the importance of a feature, especially if it is involved in complex interactions with other features. Secondly, in later training epochs, the absolute weights corresponding to regrown neurons are compared with those of neurons that have been in the network for longer. Therefore, features are compared while being given different times to grow their weights. To mitigate both of these drawbacks, we propose to regrow features randomly and to use a metric of the change a feature induces in the network over the first few mini-batches after it enters the network for pruning.

3 THE RELCHANET ALGORITHM

We propose the RelChaNet algorithm for neural network feature selection. This section walks through the pseudocode in Algorithm 1 and explains its rationale. Figure 1 illustrates the core loop of using a relative change metric to select features. RelChaNet is implemented using PyTorch (Paszke et al., 2019) and is available as a Python package in our GitHub repository.

The algorithm assumes a multi-layer perceptron (MLP) with a feed-forward architecture and is integrated into the backpropagation training using the Adam optimizer (Goodfellow et al., 2016; Kingma & Ba, 2015). This implies the adoption of the hyperparameters of learning rate, batch size,

Algorithm 1 RelChaNet

- 1: **Input.** Dataset with N features, number of selected features K , number of first hidden layer neurons n_{hidden} . Hyperparameters: Ratio of candidate features c_{ratio} , number of mini-batches n_{mb}
 - 2: **Initialize.** Number of candidate features $K_c = \text{round}(c_{\text{ratio}}(N - K))$. Network with input layer size $K + K_c$. Randomly choose features to populate the input layer. Score vector $\mathbf{s} \in \mathbb{R}^{K+K_c}$, high score vector $\mathbf{h} \in \mathbb{R}^N$. First layer gradients $\mathbf{G}^{(1)}$ and gradient sum matrix \mathbf{S} : $\mathbf{G}^{(1)}, \mathbf{S} \in \mathbb{R}^{(K+K_c) \times n_{\text{hidden}}}$
 - 3: **while** training not stopped **do**
 - 4: $\mathbf{S} = 0$
 - 5: **for** n_{mb} mini-batches **do**
 - 6: *Feed-forward step and backpropagation using a mini-batch of data*
 - 7: $\mathbf{S} = \mathbf{S} + \mathbf{G}^{(1)}$
 - 8: **end for**
 - 9: $\mathbf{s}_i = \sum_{j=1}^{n_{\text{hidden}}} |\mathbf{S}_{ij}|$ for $i \in \{1, \dots, K + K_c\}$
 - 10: $\mathbf{s} = (\mathbf{s} - \text{Mean}(\mathbf{s}))/\text{SD}(\mathbf{s})$
 - 11: Update the high scores \mathbf{h} for all candidate features if the corresponding entry in \mathbf{s} is larger
 - 12: Rotate features in the input layer: The top K features according to the high scores \mathbf{h} remain in the network and K_c candidate features are drawn randomly
 - 13: Initialize the first layer weights of all input neurons that correspond to candidates by drawing from $U(-10^{-8}, 10^{-8})$. Initialize the optimizer
 - 14: **end while**
-

and number of hidden layers and their sizes. The size of the input layer is based on the desired number of selected features K plus a percentage c_{ratio} of the remaining features, K_c , which will be referred to as candidates.

Algorithm 1 outlines the neural network training, where Step 6 represents the usual feed-forward step and backpropagation. In the surrounding loop in Steps 5-8, which runs for n_{mb} mini-batches, the first layer gradients $\mathbf{G}^{(1)}$ are aggregated by simple addition (see also Figure 1). Afterwards, Steps 9 and 10 serve to normalize the gradient sums, resulting in one relative change score s_i for each input neuron i . This is done by first taking the L^1 norm for each row of \mathbf{S} and then z-standardizing the resulting vector. For all candidates, these scores are used in Step 11 to update their respective high scores in vector \mathbf{h} . When passing this step for the first time, all neurons in the input layer are treated as candidates. The input layer is rotated in Step 12, during which the K features with the highest high scores remain, and random new candidates are drawn. In Step 13, the top features retain their corresponding first layer weights, while other first layer weights are initialized to values around 0. Except for these weights from $U(-10^{-8}, 10^{-8})$ set to break symmetry between neurons (Goodfellow et al., 2016), the network at this point follows the restriction of K active neurons from Equation 1. The stopping method is left open in the algorithm. In the experiments in this paper, stopping is performed based on the loss in a set of validation data and the convergence of the top K features (see Section A.2).

The sum of the gradients across mini-batches, \mathbf{S} , is a measure of change in the corresponding network weights. If the learning rate were kept constant throughout the mini-batches, as done in Stochastic Gradient Descent, the sum of gradients would be perfectly correlated with the change in weights that occurs during Steps 5 to 8, resulting in the same relative change score \mathbf{s} . However, for the Adam optimizer used here, the learning rate varies based on the first and second-order moments of the gradients (Kingma & Ba, 2015). This motivates comparing these different change measures—the gradient sums and the weight changes—in an ablation study in Section 4.2.

Our algorithm approaches the L^0 regularization task laid out in Equation 1 by stabilizing the high score vector \mathbf{h} . At the time of each input layer rotation, the network is forced to adhere to the criterion of only K active features, after which it gets to assess additional candidates again for a few mini-batches. This gives the network some time to find and make use of complex interactions between features. The high scores \mathbf{h} , since they preserve information over time, allow a comparison of the entry performance of candidates with the entry performance of features that entered epochs ago. Specifically, in later epochs of training, good candidates do not need to surpass the absolute first layer weights of the more established neurons.

Algorithm 2 RelChaNet flex

```
1: Initialize: Loss before the last change of the network size  $l_{\text{change}}$ , running loss  $l$ . Set the input
   layer size change direction to shrink.
2: if  $l$  has not decreased for 10 rotations then
3:   if  $l > l_{\text{change}}$  then
4:     Change the direction: shrink  $\leftrightarrow$  grow
5:   end if
6:    $l_{\text{change}} = l$ 
7:   if direction is shrink then
8:      $c_{\text{ratio}} = \max(\frac{1}{2}c_{\text{ratio}}, \frac{1}{5}\frac{K}{N-K})$ 
9:   else if direction is grow then
10:     $c_{\text{ratio}} = \min(2c_{\text{ratio}}, 1)$ 
11:  end if
12: end if
```

One drawback of this approach arises from regrown candidate neurons being chosen randomly and not selected based on a metric before entering (Step 12). Consequently, it may take many rotations of the input layer until all features had been included in the input layer at least once. This can be counteracted by increasing the c_{ratio} hyperparameter, which makes the input layer larger, or by adapting c_{ratio} throughout training.

3.1 ADAPTIVE NETWORK SIZES

To mitigate sensitivity to the input layer size set by the c_{ratio} hyperparameter, we propose an adaptive version of the algorithm that dynamically adjusts the input layer during training. The size of the input layer can shrink or grow based on the behavior of the loss function. It extends Algorithm 1 between Steps 11 and 12, i.e., prior to selecting new candidate features, and is detailed in pseudocode in Algorithm 2, RelChaNet flex.

The running loss l as well as the loss at the time of input layer change, l_{change} , can be either a training or validation loss, depending on whether the algorithm is used with a validation set. In our experiments, we use a validation set, which is detailed in Appendix A.2. A prerequisite for a size change is that the loss has not decreased for a number of neuron rotations, which is checked at Step 2. Moreover, if the current loss is larger than the loss at the time of the last input layer size change, the input layer size change direction is reversed (Steps 3-5). This is only checked for the second possible size change, since l_{change} is only defined along with the first size change. The shrinking or growing of the input layer happens in Steps 7-11, depending on the current direction. Here, the c_{ratio} hyperparameter is increased or decreased by a factor of 2 while respecting some minimum and maximum limits. The upper limit of $c_{\text{ratio}} = 1$ represents using the maximum number of candidates, $N - K$, while the lower limit ensures a minimum input layer size of $\frac{6}{5}K$.

The idea of the algorithm is that, for a well-chosen input layer size, the loss will gradually decrease. If it does not, we can try shrinking or growing the input layer. By comparing the current loss with the loss at the last size change, l_{change} , we can assess whether performance is improving in the current direction and adjust the direction if necessary.

4 EXPERIMENTS

In this section, we conduct an empirical evaluation of our proposed algorithms structured into a main experiment and additional analyses. To conserve computational resources, we replicate the experimental setup of Atashgahi et al. (2023)¹ and compare our results with those of nine state-of-the-art baseline methods reported in their work. The compared baseline methods and the RelChaNet

¹This includes code for data preprocessing, train-test split, and downstream learners, which is available at <https://github.com/zahraatashgahi/NeuroFS>. The performance of the downstream learners using all features was compared with the reported values to ensure accurate replication of the experiment setup. As detailed in our GitHub repository, this was unsuccessful for the BASEHOCK and SMK datasets, which are therefore omitted from the experiment.

Table 1: Dataset dimensions and domain

	Cases	Features	Domain	Reference
Long Datasets				
COIL-20	1440	1024	Image	Nene et al. (1996)
HAR	10299	561	Smartphone Sensor	Anguita et al. (2013)
ISOLET	7797	617	Speech	Fanty & Cole (1990)
MNIST	70000	784	Image	Deng (2012)
Fashion-MNIST	70000	784	Image	Xiao et al. (2017)
USPS	9298	256	Image	Hull (1994)
Wide Datasets				
ARCENE	200	10000	Genomics	Guyon et al. (2004)
GLA-BRA-180	180	49151	Genomics	Sun et al. (2006)
Prostate-GE	102	5966	Genomics	Nie et al. (2010)

implementations are described in Appendix A. Code for replicating the main experiment is available in our GitHub repository.

The datasets used and their dimensions are shown in Table 1. We categorize datasets as long if they have more cases than features, and vice versa as wide. The datasets all represent classification tasks and span different content domains, including speech processing (ISOLET), image recognition (MNIST), and smartphone sensor data (HAR). They are all freely available.

To ensure a fair comparison between embedded and filter methods, all experimental conditions include downstream learners. Initially, the data is split into training and test sets. Feature selection is performed using the training data, followed by training a downstream predictive model on the training data using only the selected features. The accuracy of the downstream learner is then evaluated on the test data. The number of selected features, K , varies among 25, 50, 75, and 100². The downstream learners are classifiers based on a Support Vector Machine (SVM, Chang & Lin, 2011), K-Nearest Neighbors (KNN), and ExtraTrees (ET, Geurts et al., 2006). The SVM classifier is used for all values of K , while KNN and ET are only used for $K = 50$. Each condition is run five times. Experiments are conducted on an NVIDIA GeForce RTX 3060 GPU with 6GB of memory.

4.1 RESULTS

Figure 2 presents a comparison of the accuracies achieved using our methods ("RCN" and "RCN flex") against the top baseline methods for the SVM downstream learner. The average accuracy by dataset is shown for all methods in Figure 3. Detailed results for each dataset, method, and value of K are provided in Table 2 in Appendix B.

According to the results, our approaches significantly outperform the baseline methods for most long datasets (first six panels in the plots). In particular, for the MNIST dataset, our flex approach achieves an average accuracy of 96.3%, significantly improving on the best previous result of 94.3%. Our methods demonstrate comparable performance to the baseline methods for the wide datasets (last three panels in the plots), but fall slightly behind for the GLA-BRA-180 dataset. The RCN and RCN flex approaches perform similarly in all conditions except for the ARCENE dataset, where the RCN approach performs notably worse than the top baselines.

We also evaluated two additional downstream learners, KNN and ET, under the condition of $K = 50$ selected variables (see Table 3 in Appendix B). The results are very similar to those obtained with the SVM classifier, indicating that the selected feature sets are valuable across multiple downstream learners.

²Atashgahi et al. (2023) also used higher values for K which are omitted in this study since there was little variance in the results between the different methods.

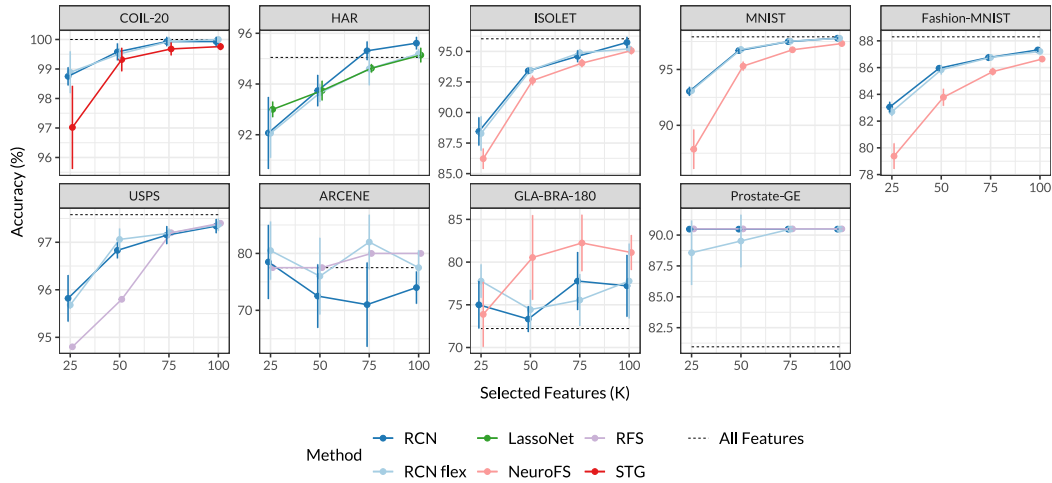


Figure 2: Resulting accuracy for the studied methods by dataset and number of selected features K using the SVM downstream learner. Our proposed methods are "RCN" and "RCN flex". For visual clarity, only the baseline method with the highest average accuracy for each dataset is shown. "All Features" is the accuracy using all features in the dataset. Error bars indicate the standard deviation. Results for the baseline methods are reproduced from [Atashgahi et al. \(2023\)](#).

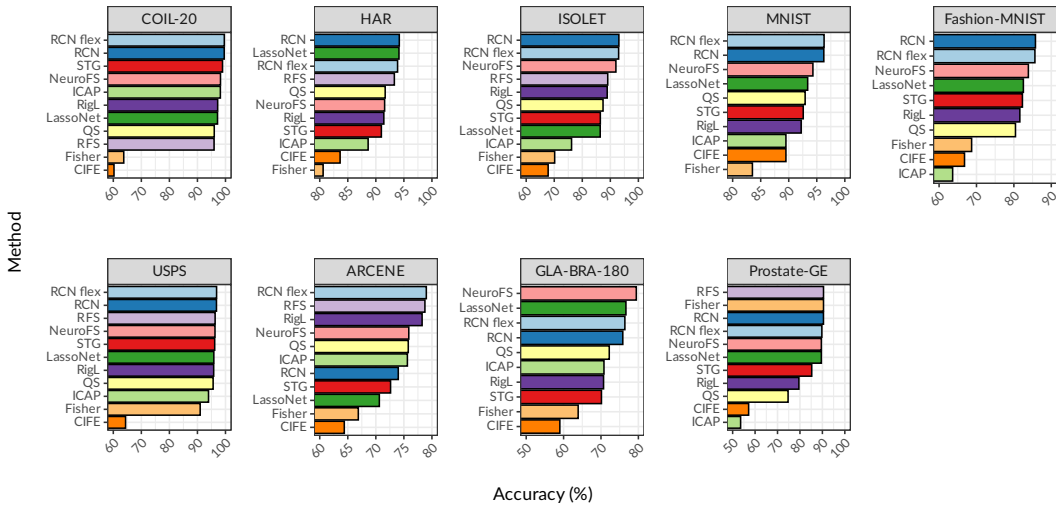


Figure 3: Average accuracy by dataset for the studied methods using the SVM downstream learner. Our proposed methods are "RCN" and "RCN flex". Results for the baseline methods are reproduced from [Atashgahi et al. \(2023\)](#).

4.2 ADDITIONAL ANALYSES

Computational efficiency. We examine the comparative computational costs with two other approaches, NeuroFS and LassoNet. Both are well-performing sparse and dense neural network based methods, respectively. One drawback of our approach is that, since candidate features are chosen randomly, it generally requires more training epochs than other approaches to ensure that all features get the chance to enter the network. This motivates comparing the overall runtime of the approaches.

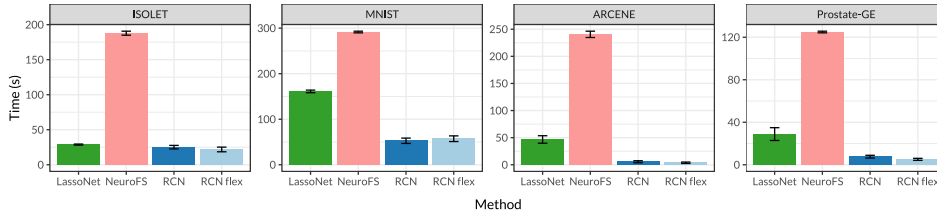


Figure 4: Wall-clock run time for the studied methods by dataset. All conditions use $K = 50$ selected features and are repeated five times. The error bars indicate the standard deviation.

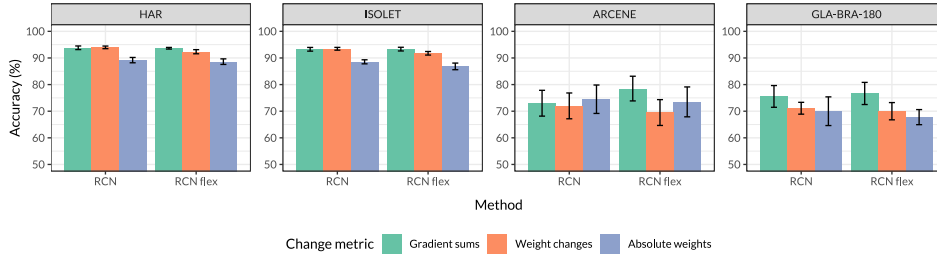


Figure 5: Resulting accuracy for the studied change metrics by RCN method and dataset for $K = 50$ selected features using the SVM downstream learner. The error bars indicate the standard deviation.

We measure the wall-clock time for selecting $K = 50$ features, using two wide and two long datasets, with settings otherwise as in the main experiment. For NeuroFS, we use the setup from the original publication: a 3-layer sparse MLP with 1000 neurons in each layer, limiting the training epochs to 100. For LassoNet, we use the same MLP architecture as for RelChaNet, i.e., one hidden layer with 100 neurons. We keep all other settings at the LassoNet package defaults³. Each condition is run five times.

The results are shown in Figure 4. They demonstrate that our approach is significantly more efficient than NeuroFS for the studied datasets and more efficient than LassoNet for three of the four conditions. One possible explanation is that the larger number of epochs required by our approach may be offset by a comparatively small computational overhead. The RCN and RCN flex approaches take a similar amount of time.

Ablation study: Change metrics. We compare the performance of RelChaNet under different change metrics. Specifically, we evaluate the gradient sums used in RelChaNet against using weight changes or absolute weights. In both cases, the calculation of \mathcal{S} is modified immediately before Step 9 of Algorithm 1. For the weight changes, we set $\mathcal{S} = \mathbf{W}^{(1)} - \mathbf{W}_{\text{old}}^{(1)}$, where $\mathbf{W}_{\text{old}}^{(1)}$ are the first layer weights at the time of the last rotation. For the absolute weights, we simply set \mathcal{S} equal to the first layer weights, $\mathcal{S} = \mathbf{W}^{(1)}$. We use four datasets, two long and two wide, and $K = 50$ selected features, keeping all other properties the same as in the main experiment.

Figure 5 shows the results. For the long datasets (two panels on the left), the gradient sums and weight changes produce comparable results, surpassing the performance of absolute weights. For the wide datasets (right two panels), the gradient sums show superior performance, while the other two approaches exhibit similar effectiveness. In summary, under the studied conditions, gradient sums are the most effective metric for measuring relative change within the RelChaNet algorithm.

Hyperparameters. We investigate the role of the hyperparameters c_{ratio} and n_{mb} . Generally, c_{ratio} determines the percentage of features included in the network in addition to the K selected features, while n_{mb} specifies the number of mini-batches after which scores are computed and features are

³The LassoNet package is available at <https://github.com/lasso-net/lassonet>.

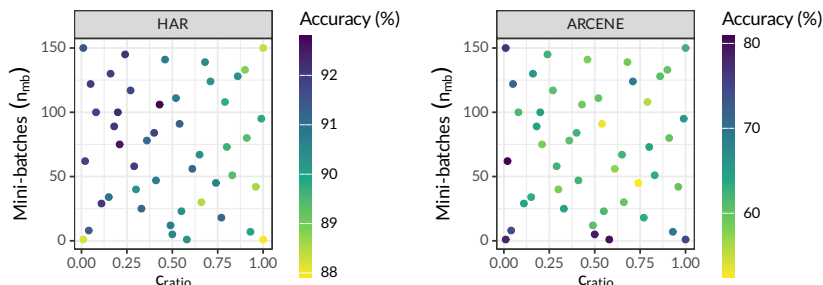


Figure 6: Accuracy using RelChaNet feature selection by hyperparameters c_{ratio} and n_{mb} for two datasets and $K = 25$ selected features. Each point represents the average of three runs.

rotated. We use a long and a wide dataset, HAR and ARCENE, $K = 25$, and keep all other properties consistent with the main experiment. We let c_{ratio} vary between 0.01 and 1 and n_{mb} between 1 and 150. As studied hyperparameter sets we include the two configurations from our experiment: ($c_{\text{ratio}} = 0.2$, $n_{\text{mb}} = 100$) for the long datasets and ($c_{\text{ratio}} = 0.5$, $n_{\text{mb}} = 5$) for the wide datasets. Additionally, we include the four corners of the hyperparameter space and draw 40 pseudo-random sets of configurations from a Halton sequence. Each resulting condition is run three times, and the accuracy is averaged.

The results are illustrated in Figure 6. For the long HAR dataset (left panel), the combination of low c_{ratio} and high n_{mb} yields strong results. In contrast, for the ARCENE dataset (right panel), configurations with low n_{mb} generally perform well. A combination of low c_{ratio} and higher n_{mb} may also be effective. This highlights that hyperparameters must be selected differently for different datasets, with a comparatively narrower range working well for wide datasets.

5 DISCUSSION

In this paper, we introduce a novel feature selection algorithm aimed at enhancing the predictive performance and interpretability of predictive models. Our approach incorporates neuron pruning and regrowth from the sparse neural network literature into a dense neural network framework. RelChaNet uses a relative change metric for pruning, which measures the relative change induced in a network after a feature enters, while neurons are randomly regrown. Extensive experiments demonstrate that our method, along with an extension featuring an adaptive input layer, consistently outperforms state-of-the-art techniques on datasets characterized by a higher number of cases than features. For datasets with more features than cases, the performance is comparable to previous approaches.

The primary limitation of our approach lies in its theoretical disadvantage in computational efficiency. This is due in part to the reliance on a dense network, which typically has higher computational training costs than sparse networks with the same number of layers and neurons. Additionally, regrowing neurons randomly necessitates either a large input layer or longer training. However, our experiment demonstrates that these challenges can be mitigated by employing a small neural network architecture without compromising feature selection performance. Furthermore, the efficiency was found to be competitive with another dense approach. It is important to note, however, that this may not generalize to scenarios beyond those studied.

We see many potential directions for future research. One avenue is to integrate our pruning and regrowth protocol into sparse neural networks. This could be applied to the input layer for feature selection, or extended to other layers for general sparse neural network training. Another direction is to explore the utility of our approach for interpretable machine learning. For instance, the values in the high score vector \mathbf{h} could be evaluated as a measure of variable importance.

REPRODUCIBILITY STATEMENT

We include the source code of our method in the form of a Python package, as well as code to reproduce the main experiment results at <https://github.com/flxzimmer/relchanet>.

ACKNOWLEDGEMENTS

Many thanks to Rudolf Debelak for his helpful feedback and thorough review.

REFERENCES

- D. Anguita, Alessandro Ghio, L. Oneto, Xavier Parra, and Jorge Luis Reyes-Ortiz. A public domain dataset for human activity recognition using smartphones. In *The European Symposium on Artificial Neural Networks*, 2013.
- Zahra Atashgahi, Ghada Sokar, Tim Van Der Lee, Elena Mocanu, Decebal Constantin Mocanu, Raymond Veldhuis, and Mykola Pechenizkiy. Quick and robust feature selection: The strength of energy-efficient sparse training for autoencoders. *Machine Learning*, 111(1):377–414, January 2022. ISSN 0885-6125, 1573-0565. doi:[10.1007/s10994-021-06063-x](https://doi.org/10.1007/s10994-021-06063-x).
- Zahra Atashgahi, Xuhao Zhang, Neil Kichler, Shiwei Liu, Lu Yin, Mykola Pechenizkiy, Raymond Veldhuis, and Decebal Constantin Mocanu. Supervised feature selection with neuron evolution in sparse neural networks. *Transactions on Machine Learning Research*, 2023. ISSN 2835-8856.
- Zahra Atashgahi, Tennison Liu, Mykola Pechenizkiy, Raymond Veldhuis, Decebal Constantin Mocanu, and Mihaela van der Schaar. Unveiling the Power of Sparse Neural Networks for Feature Selection. *arXiv preprint arXiv:2408.04583*, 2024.
- Andrea Bommert, Xudong Sun, Bernd Bischl, Jörg Rahnenführer, and Michel Lang. Benchmark for filter methods for feature selection in high-dimensional classification data. *Computational Statistics & Data Analysis*, 143:106839, March 2020. ISSN 0167-9473. doi:[10.1016/j.csda.2019.106839](https://doi.org/10.1016/j.csda.2019.106839).
- Chih-Chung Chang and Chih-Jen Lin. LIBSVM: A library for support vector machines. *ACM Transactions on Intelligent Systems and Technology*, 2(3):1–27, April 2011. ISSN 2157-6904, 2157-6912. doi:[10.1145/1961189.1961199](https://doi.org/10.1145/1961189.1961199).
- Valeriia Cherepanova, Roman Levin, Gowthami Somepalli, Jonas Geiping, C. Bayan Bruss, Andrew G Wilson, Tom Goldstein, and Micah Goldblum. A Performance-Driven Benchmark for Feature Selection in Tabular Deep Learning. In A. Oh, T. Neumann, A. Globerson, K. Saenko, M. Hardt, and S. Levine (eds.), *Advances in Neural Information Processing Systems*, volume 36, pp. 41956–41979. Curran Associates, Inc., 2023.
- Li Deng. The MNIST database of handwritten digit images for machine learning research [best of the web]. *IEEE Signal Processing Magazine*, 29:141–142, 2012.
- Utku Evci, Trevor Gale, Jacob Menick, Pablo Samuel Castro, and Erich Elsen. Rigging the Lottery: Making All Tickets Winners. In Hal Daumé III and Aarti Singh (eds.), *Proceedings of the 37th International Conference on Machine Learning*, volume 119 of *Proceedings of Machine Learning Research*, pp. 2943–2952. PMLR, July 2020.
- Mark Fanty and Ronald Cole. Spoken letter recognition. In *Proceedings of the 3rd International Conference on Neural Information Processing Systems, NIPS’90*, pp. 220–226, San Francisco, CA, USA, 1990. Morgan Kaufmann Publishers Inc. ISBN 1-55860-184-8.
- Pierre Geurts, Damien Ernst, and Louis Wehenkel. Extremely randomized trees. *Machine Learning*, 63(1):3–42, April 2006. ISSN 0885-6125, 1573-0565. doi:[10.1007/s10994-006-6226-1](https://doi.org/10.1007/s10994-006-6226-1).
- Ian Goodfellow, Yoshua Bengio, and Aaron Courville. *Deep Learning*. The MIT Press, Cambridge, Massachusetts, November 2016. ISBN 978-0-262-03561-3.

-
- Quanquan Gu, Zhenhui Li, and Jiawei Han. Generalized Fisher score for feature selection. In *Proceedings of the Twenty-Seventh Conference on Uncertainty in Artificial Intelligence, UAI'11*, pp. 266–273, Arlington, Virginia, USA, 2011. AUAI Press. ISBN 978-0-9749039-7-2.
- Isabelle Guyon, Steve Gunn, Asa Ben-Hur, and Gideon Dror. Arcene. *UCI Machine Learning Repository*, 2004. doi:[10.24432/C58P55](https://doi.org/10.24432/C58P55).
- Torsten Hoefer, Dan Alistarh, Tal Ben-Nun, Nikoli Dryden, and Alexandra Peste. Sparsity in deep learning: Pruning and growth for efficient inference and training in neural networks. *Journal of Machine Learning Research*, 22(241):1–124, 2021.
- J. J. Hull. A database for handwritten text recognition research. *IEEE Transactions on Pattern Analysis and Machine Intelligence*, 16(5):550–554, May 1994. ISSN 0162-8828. doi:[10.1109/34.291440](https://doi.org/10.1109/34.291440).
- Aleks Jakulin. *Machine Learning Based on Attribute Interactions*. PhD thesis, Univerza v Ljubljani, 2005.
- Diederik P. Kingma and Jimmy Ba. Adam: A method for stochastic optimization. In Yoshua Bengio and Yann LeCun (eds.), *3rd International Conference on Learning Representations, ICLR 2015, San Diego, CA, USA, May 7-9, 2015, Conference Track Proceedings*, 2015.
- Ismael Lemhadri, Feng Ruan, Louis Abraham, and Robert Tibshirani. LassoNet: A neural network with feature sparsity. *Journal of Machine Learning Research*, 22(127):1–29, 2021.
- Jundong Li, Kewei Cheng, Suhang Wang, Fred Morstatter, Robert P. Trevino, Jiliang Tang, and Huan Liu. Feature Selection: A Data Perspective. *ACM Computing Surveys*, 50(6):1–45, November 2018. ISSN 0360-0300, 1557-7341. doi:[10.1145/3136625](https://doi.org/10.1145/3136625).
- Dahua Lin and Xiaoou Tang. Conditional Infomax Learning: An Integrated Framework for Feature Extraction and Fusion. In Aleš Leonardis, Horst Bischof, and Axel Pinz (eds.), *Computer Vision – ECCV 2006*, volume 3951, pp. 68–82. Springer Berlin Heidelberg, Berlin, Heidelberg, 2006. ISBN 978-3-540-33832-1. doi:[10.1007/11744023_6](https://doi.org/10.1007/11744023_6).
- Kaiting Liu, Zahra Atashgahi, Ghada Sokar, Mykola Pechenizkiy, and Decebal Constantin Mocanu. Supervised Feature Selection via Ensemble Gradient Information from Sparse Neural Networks. In *International Conference on Artificial Intelligence and Statistics*, pp. 3952–3960. PMLR, 2024.
- Decebal Constantin Mocanu, Elena Mocanu, Peter Stone, Phuong H. Nguyen, Madeleine Gibescu, and Antonio Liotta. Scalable training of artificial neural networks with adaptive sparse connectivity inspired by network science. *Nature Communications*, 9(1):2383, June 2018. ISSN 2041-1723. doi:[10.1038/s41467-018-04316-3](https://doi.org/10.1038/s41467-018-04316-3).
- Pavlo Molchanov, Arun Mallya, Stephen Tyree, Iuri Frosio, and Jan Kautz. Importance Estimation for Neural Network Pruning. In *2019 IEEE/CVF Conference on Computer Vision and Pattern Recognition (CVPR)*, pp. 11256–11264, Long Beach, CA, USA, June 2019. IEEE. ISBN 978-1-72813-293-8. doi:[10.1109/CVPR.2019.01152](https://doi.org/10.1109/CVPR.2019.01152).
- Samer A. Nene, Shree K. Nayar, and Hiroshi Murase. Columbia object image library (COIL-20). Technical Report CUCS-005-96, Department of Computer Science, Columbia University, February 1996.
- Feiping Nie, Heng Huang, Xiao Cai, and Chris Ding. Efficient and robust feature selection via joint l_2, l_1 -norms minimization. In J. Lafferty, C. Williams, J. Shawe-Taylor, R. Zemel, and A. Culotta (eds.), *Advances in Neural Information Processing Systems*, volume 23. Curran Associates, Inc., 2010.
- Adam Paszke, Sam Gross, Francisco Massa, Adam Lerer, James Bradbury, Gregory Chanan, Trevor Killeen, Zeming Lin, Natalia Gimelshein, Luca Antiga, Alban Desmaison, Andreas Kopf, Edward Yang, Zachary DeVito, Martin Raison, Alykhan Tejani, Sasank Chilamkurthy, Benoit Steiner, Lu Fang, Junjie Bai, and Soumith Chintala. PyTorch: An imperative style, high-performance deep learning library. In H. Wallach, H. Larochelle, A. Beygelzimer, F. dAlché-Buc, E. Fox, and R. Garnett (eds.), *Advances in Neural Information Processing Systems*, volume 32. Curran Associates, Inc., 2019.

-
- Mehrdad Rostami, Kamal Berahmand, Elahe Nasiri, and Saman Forouzandeh. Review of swarm intelligence-based feature selection methods. *Engineering Applications of Artificial Intelligence*, 100:104210, April 2021. ISSN 09521976. doi:[10.1016/j.engappai.2021.104210](https://doi.org/10.1016/j.engappai.2021.104210).
- Ghada Sokar, Zahra Atashgahi, Mykola Pechenizkiy, and Decebal Constantin Mocanu. Where to pay attention in sparse training for feature selection? In *Proceedings of the 36th International Conference on Neural Information Processing Systems, Nips '22*, Red Hook, NY, USA, 2024. Curran Associates Inc. ISBN 978-1-71387-108-8.
- Lixin Sun, Ai-Min Hui, Qin Su, Alexander Vortmeyer, Yuri Kotliarov, Sandra Pastorino, Antonino Passaniti, Jayant Menon, Jennifer Walling, Rolando Bailey, Marc Rosenblum, Tom Mikkelsen, and Howard A. Fine. Neuronal and glioma-derived stem cell factor induces angiogenesis within the brain. *Cancer Cell*, 9(4):287–300, April 2006. ISSN 15356108. doi:[10.1016/j.ccr.2006.03.003](https://doi.org/10.1016/j.ccr.2006.03.003).
- Robert Tibshirani. Regression shrinkage and selection via the lasso. *Journal of the Royal Statistical Society. Series B (Methodological)*, 58(1):267–288, 1996. ISSN 00359246.
- Han Xiao, Kashif Rasul, and Roland Vollgraf. Fashion-MNIST: A Novel Image Dataset for Benchmarking Machine Learning Algorithms. *arXiv preprint arXiv:1708.07747*, 2017.
- Yutaro Yamada, Ofir Lindenbaum, Sahand Negahban, and Yuval Kluger. Feature selection using stochastic gates. In Hal Daumé III and Aarti Singh (eds.), *Proceedings of the 37th International Conference on Machine Learning*, volume 119 of *Proceedings of Machine Learning Research*, pp. 10648–10659. PMLR, 2020.

A EXPERIMENTAL SETUP

A.1 BASELINES

The methods compared against our approach are as follows. Their specific implementations are detailed in [Atashgahi et al. \(2023\)](#):

- Fisher Score ([Gu et al., 2011](#)): A classic filter method that selects feature sets based on their ability to separate data points.
- CIFE (Conditional Infomax Feature Extraction, [Lin & Tang, 2006](#)): A filter method that aims to maximize the class-relevant information of the feature set.
- ICAP (Interaction Capping Criterion, [Jakulin, 2005](#)): A filter method that considers the complementary relationship between features.
- RFS (Robust Feature Selection, [Nie et al., 2010](#)): A method embedded in regression that uses joint L^1 and L^2 regularization of the weights.
- QS (Quick Selection, [Atashgahi et al., 2022](#)): A method embedded in sparse neural networks that combines denoising autoencoders and the L^1 norm of first layer neuron weights.
- STG (Stochastic Gates, [Yamada et al., 2020](#)): A method embedded in neural networks that controls the input layer neurons using a trainable probabilistic gate.
- LassoNet ([Lemhadri et al., 2021](#)): A method embedded in neural networks that adds a regularized residual connection from the input layer to the output. The residual connection controls the sizes of first layer weights.
- RigL ([Evcı et al., 2020](#)): A method embedded in sparse neural networks that rotates features by pruning based on parameter weights and regrowing based on gradients. Feature selection can be performed by investigating first layer weights after training ([Atashgahi et al., 2023](#)).
- NeuroFS ([Atashgahi et al., 2023](#)): A method embedded in sparse neural networks that extends the ideas used in RigL to input neurons.

A.2 RELCHANET SETUP

The parameters used for RelChaNet in the main experiment are as follows. We employ a single hidden layer neural network with 100 neurons and a ReLU activation function. For training, we use a batch size of 1024 and a learning rate of 0.001 for the Adam optimizer. If there are fewer cases in the dataset, full batches are used instead. The hyperparameters specific to our method are: $c_{\text{ratio}} = 0.2$ and $n_{\text{mb}} = 100$ for long datasets, and $c_{\text{ratio}} = 0.5$ and $n_{\text{mb}} = 5$ for wide datasets. Stopping is based on a combination of validation loss and the identified feature set. For this, the training data is split again into a training and a validation set. Training continues on the training set until the validation loss does not decrease for 100 input layer rotations or the set of K features with the highest values in \mathbf{h} remains unchanged for 100 rotations. Afterwards, the training is again performed on the complete training data for the determined number of rotations. For the flex algorithm, during this final training phase, the input layer is scaled from its initial size to the final size using a total of ten size change steps.

B DETAILED RESULTS

Table 2: Resulting accuracy of the studied methods for different numbers of selected features K and datasets using the SVM downstream learner. Our proposed methods are "RCN" and "RCN flex". "All" is the accuracy using all features in the dataset. The best and second-best methods for each combination of K and dataset are marked in bold and underlined, respectively. Entries represent the mean \pm standard deviation of the downstream learner accuracy across five runs. Results for the baseline methods are reproduced from [Atashgahi et al. \(2023\)](#).

	COIL-20	HAR	ISOLET	MNIST	Fashion-MNIST	USPS	ARCENE	GLA-BRA-180	Prostate-GE
All	100.00	95.05	96.03	97.92	88.30	97.58	77.50	72.22	80.95
K = 25									
NeuroFS	95.86 \pm 1.31	87.46 \pm 0.79	86.22 \pm 0.84	87.86 \pm 1.77	79.38 \pm 0.96	93.98 \pm 0.87	63.00 \pm 4.85	73.88 \pm 3.80	88.58 \pm 2.35
LassoNet	92.72 \pm 0.85	93.00 \pm 0.31	76.48 \pm 0.39	86.40 \pm 1.26	78.68 \pm 0.55	94.04 \pm 0.38	69.00 \pm 2.55	<u>76.12 \pm 4.19</u>	88.58 \pm 2.35
STG	97.02 \pm 1.41	87.48 \pm 0.80	77.16 \pm 4.34	85.24 \pm 1.89	77.44 \pm 0.53	94.04 \pm 0.46	69.00 \pm 5.15	67.22 \pm 4.78	85.72 \pm 3.00
QS	91.00 \pm 4.21	87.14 \pm 1.74	72.56 \pm 6.53	85.25 \pm 1.47	71.57 \pm 1.97	93.00 \pm 0.81	73.75 \pm 8.20	69.45 \pm 2.75	71.43 \pm 12.16
Fisher	24.70 \pm 0.00	77.10 \pm 0.00	57.40 \pm 0.00	74.40 \pm 0.00	53.10 \pm 0.00	82.00 \pm 0.00	65.00 \pm 0.00	58.30 \pm 0.00	90.50 \pm 0.00
CIFE	50.70 \pm 0.00	80.20 \pm 0.00	56.00 \pm 0.00	80.90 \pm 0.00	63.40 \pm 0.00	50.20 \pm 0.00	67.50 \pm 0.00	61.10 \pm 0.00	61.90 \pm 0.00
ICAP	94.40 \pm 0.00	84.50 \pm 0.00	67.10 \pm 0.00	81.60 \pm 0.00	50.10 \pm 0.00	89.90 \pm 0.00	77.50 \pm 0.00	69.40 \pm 0.00	47.60 \pm 0.00
RFS	88.20 \pm 0.00	88.90 \pm 0.00	76.50 \pm 0.00	-	-	94.80 \pm 0.00	77.50 \pm 0.00	-	90.50 \pm 0.00
RigL	92.38 \pm 3.20	86.46 \pm 1.47	79.98 \pm 2.25	82.06 \pm 0.99	74.12 \pm 1.59	93.10 \pm 0.62	74.50 \pm 4.30	66.10 \pm 3.22	78.08 \pm 6.46
RCN	<u>98.75 \pm 0.31</u>	<u>92.07 \pm 1.42</u>	88.45 \pm 1.16	<u>93.04 \pm 0.41</u>	83.05 \pm 0.40	95.82 \pm 0.49	<u>78.50 \pm 6.52</u>	75.00 \pm 2.78	90.48 \pm 0.00
RCN flex	98.89 \pm 0.71	92.06 \pm 0.97	<u>88.28 \pm 1.41</u>	93.10 \pm 0.25	<u>82.70 \pm 0.32</u>	<u>95.68 \pm 0.08</u>	80.50 \pm 5.12	<u>77.78 \pm 1.96</u>	88.57 \pm 2.61
K = 50									
NeuroFS	98.78 \pm 0.29	91.46 \pm 0.72	92.62 \pm 0.40	95.30 \pm 0.41	83.78 \pm 0.64	96.78 \pm 0.17	76.50 \pm 2.55	80.54 \pm 4.96	90.50 \pm 0.00
LassoNet	97.16 \pm 1.06	<u>93.74 \pm 0.39</u>	84.90 \pm 0.22	94.46 \pm 0.21	82.58 \pm 0.10	95.94 \pm 0.15	71.00 \pm 2.00	<u>74.46 \pm 4.78</u>	88.58 \pm 2.35
STG	99.32 \pm 0.40	<u>91.22 \pm 1.23</u>	85.82 \pm 2.83	93.20 \pm 0.62	82.36 \pm 0.52	96.62 \pm 0.34	71.00 \pm 2.55	70.00 \pm 4.08	84.78 \pm 3.55
QS	96.52 \pm 1.53	91.96 \pm 1.04	89.78 \pm 1.80	93.62 \pm 0.49	80.82 \pm 0.51	95.52 \pm 0.27	74.38 \pm 4.80	72.20 \pm 2.80	76.20 \pm 7.53
Fisher	74.00 \pm 0.00	79.80 \pm 0.00	67.40 \pm 0.00	81.90 \pm 0.00	67.80 \pm 0.00	91.00 \pm 0.00	67.50 \pm 0.00	63.90 \pm 0.00	<u>90.50 \pm 0.00</u>
CIFE	59.40 \pm 0.00	84.20 \pm 0.00	59.80 \pm 0.00	89.30 \pm 0.00	66.90 \pm 0.00	61.30 \pm 0.00	52.50 \pm 0.00	58.30 \pm 0.00	47.60 \pm 0.00
ICAP	99.30 \pm 0.00	88.70 \pm 0.00	75.10 \pm 0.00	89.00 \pm 0.00	59.50 \pm 0.00	95.20 \pm 0.00	70.00 \pm 0.00	72.20 \pm 0.00	57.10 \pm 0.00
RFS	95.80 \pm 0.00	94.00 \pm 0.00	91.50 \pm 0.00	-	-	95.80 \pm 0.00	77.50 \pm 0.00	-	90.50 \pm 0.00
RigL	97.86 \pm 1.32	91.82 \pm 0.30	89.58 \pm 1.24	93.94 \pm 0.63	81.92 \pm 0.87	96.04 \pm 0.58	<u>77.00 \pm 3.32</u>	70.54 \pm 4.16	79.06 \pm 7.11
RCN	99.58 \pm 0.29	93.74 \pm 0.62	93.41 \pm 0.25	<u>96.69 \pm 0.19</u>	85.95 \pm 0.22	<u>96.83 \pm 0.17</u>	72.50 \pm 5.59	73.33 \pm 1.52	90.48 \pm 0.00
RCN flex	<u>99.51 \pm 0.19</u>	93.65 \pm 0.36	93.46 \pm 0.19	96.79 \pm 0.11	<u>85.84 \pm 0.36</u>	97.06 \pm 0.23	76.00 \pm 6.75	74.44 \pm 2.32	89.52 \pm 2.13
K = 75									
NeuroFS	99.06 \pm 0.12	93.16 \pm 0.79	94.04 \pm 0.34	96.76 \pm 0.22	85.70 \pm 0.28	97.06 \pm 0.15	82.00 \pm 4.00	82.24 \pm 3.31	89.54 \pm 1.92
LassoNet	99.46 \pm 0.35	94.62 \pm 0.17	91.00 \pm 0.62	96.00 \pm 0.09	83.92 \pm 0.13	96.36 \pm 0.08	70.50 \pm 2.45	76.64 \pm 5.44	90.50 \pm 0.00
STG	99.68 \pm 0.22	92.42 \pm 1.11	90.10 \pm 2.17	95.52 \pm 0.22	84.14 \pm 0.43	96.88 \pm 0.23	75.00 \pm 2.74	71.08 \pm 1.37	84.78 \pm 3.55
QS	98.17 \pm 1.16	93.50 \pm 0.77	93.04 \pm 0.46	95.98 \pm 0.33	83.80 \pm 0.53	96.85 \pm 0.05	76.88 \pm 2.72	73.60 \pm 1.40	72.62 \pm 9.78
Fisher	76.00 \pm 0.00	81.70 \pm 0.00	76.00 \pm 0.00	87.10 \pm 0.00	74.30 \pm 0.00	94.40 \pm 0.00	70.00 \pm 0.00	66.70 \pm 0.00	<u>90.50 \pm 0.00</u>
CIFE	63.20 \pm 0.00	84.80 \pm 0.00	74.30 \pm 0.00	92.70 \pm 0.00	67.70 \pm 0.00	68.00 \pm 0.00	72.50 \pm 0.00	58.30 \pm 0.00	47.60 \pm 0.00
ICAP	99.00 \pm 0.00	89.20 \pm 0.00	79.70 \pm 0.00	92.40 \pm 0.00	67.20 \pm 0.00	95.30 \pm 0.00	72.50 \pm 0.00	72.20 \pm 0.00	57.10 \pm 0.00
RFS	99.70 \pm 0.00	<u>94.90 \pm 0.00</u>	93.90 \pm 0.00	-	-	97.20 \pm 0.00	80.00 \pm 0.00	-	90.50 \pm 0.00
RigL	99.20 \pm 0.43	93.34 \pm 0.47	92.32 \pm 0.56	95.98 \pm 0.51	84.52 \pm 0.72	96.90 \pm 0.24	81.50 \pm 4.64	72.22 \pm 4.98	79.06 \pm 8.83
RCN	99.93 \pm 0.16	95.31 \pm 0.37	94.60 \pm 0.49	<u>97.49 \pm 0.13</u>	<u>86.75 \pm 0.25</u>	97.15 \pm 0.19	71.00 \pm 7.42	<u>77.78 \pm 3.40</u>	90.48 \pm 0.00
RCN flex	<u>99.93 \pm 0.16</u>	94.60 \pm 0.65	94.88 \pm 0.31	97.53 \pm 0.11	86.76 \pm 0.14	<u>97.19 \pm 0.10</u>	82.00 \pm 4.81	75.56 \pm 3.04	90.48 \pm 0.00
K = 100									
NeuroFS	99.18 \pm 0.50	94.18 \pm 0.29	95.06 \pm 0.31	97.32 \pm 0.17	86.64 \pm 0.21	97.22 \pm 0.12	<u>82.00 \pm 1.87</u>	81.12 \pm 2.05	89.54 \pm 1.92
LassoNet	99.30 \pm 0.00	95.14 \pm 0.29	93.18 \pm 0.22	96.64 \pm 0.14	84.98 \pm 0.18	97.04 \pm 0.12	72.00 \pm 4.30	<u>79.46 \pm 2.83</u>	90.50 \pm 0.00
STG	99.76 \pm 0.12	92.82 \pm 0.74	92.64 \pm 0.56	96.38 \pm 0.35	85.20 \pm 0.58	97.08 \pm 0.18	75.50 \pm 3.67	72.20 \pm 3.07	85.72 \pm 3.00
QS	98.28 \pm 1.15	94.06 \pm 0.48	94.22 \pm 0.28	96.85 \pm 0.09	85.52 \pm 0.15	97.00 \pm 0.14	78.12 \pm 1.08	73.60 \pm 1.40	78.58 \pm 9.82
Fisher	80.20 \pm 0.00	83.80 \pm 0.00	79.80 \pm 0.00	90.70 \pm 0.00	79.60 \pm 0.00	96.50 \pm 0.00	65.00 \pm 0.00	66.70 \pm 0.00	<u>90.50 \pm 0.00</u>
CIFE	67.70 \pm 0.00	85.30 \pm 0.00	81.20 \pm 0.00	95.10 \pm 0.00	69.20 \pm 0.00	78.00 \pm 0.00	65.00 \pm 0.00	58.30 \pm 0.00	71.40 \pm 0.00
ICAP	100.00 \pm 0.00	92.10 \pm 0.00	82.80 \pm 0.00	95.00 \pm 0.00	77.70 \pm 0.00	95.40 \pm 0.00	82.50 \pm 0.00	69.40 \pm 0.00	52.40 \pm 0.00
RFS	100.00 \pm 0.00	95.40 \pm 0.00	94.40 \pm 0.00	-	-	97.40 \pm 0.00	80.00 \pm 0.00	-	90.50 \pm 0.00
RigL	99.40 \pm 0.43	94.08 \pm 0.26	93.66 \pm 0.58	96.88 \pm 0.22	85.82 \pm 0.23	97.14 \pm 0.10	80.00 \pm 4.47	73.90 \pm 3.76	81.92 \pm 8.18
RCN	99.93 \pm 0.16	95.61 \pm 0.25	95.73 \pm 0.46	97.80 \pm 0.10	87.32 \pm 0.15	97.34 \pm 0.15	74.00 \pm 2.85	77.22 \pm 3.62	90.48 \pm 0.00
RCN flex	100.00 \pm 0.00	95.19 \pm 0.19	<u>95.21 \pm 0.23</u>	<u>97.79 \pm 0.07</u>	<u>87.21 \pm 0.08</u>	<u>97.37 \pm 0.13</u>	77.50 \pm 3.06	77.78 \pm 4.39	90.48 \pm 0.00

Table 3: Resulting accuracy of the studied methods for different downstream learners and datasets using $K = 50$ selected features. Our proposed methods are "RCN" and "RCN flex". "All" is the accuracy using all features in the dataset. The best and second-best methods for each combination of learner and dataset are marked in bold and underlined, respectively. Entries represent the mean \pm standard deviation of the downstream learner accuracy across five runs. Results for the baseline methods are reproduced from [Atashgahi et al. \(2023\)](#).

	COIL-20	HAR	ISOLET	MNIST	Fashion-MNIST	USPS	ARCENE	GLA-BRA-180	Prostate-GE
Learner: ET									
All	100.00 \pm 0.00	93.53 \pm 0.15	94.05 \pm 0.32	97.10 \pm 0.05	87.19 \pm 0.13	96.29 \pm 0.16	79.50 \pm 4.85	75.00 \pm 4.97	88.57 \pm 3.81
NeuroFS	99.94 \pm 0.12	85.48 \pm 1.46	91.46 \pm 0.73	93.68 \pm 0.43	84.26 \pm 0.55	95.44 \pm 0.27	75.00 \pm 5.24	75.46 \pm 6.71	90.50 \pm 0.00
LassoNet	99.76 \pm 0.12	91.12 \pm 0.30	84.94 \pm 0.62	92.96 \pm 0.15	83.68 \pm 0.13	94.86 \pm 0.22	73.50 \pm 4.64	76.12 \pm 3.80	89.54 \pm 1.92
STG	100.00 \pm 0.00	88.68 \pm 0.42	88.50 \pm 2.15	90.38 \pm 0.42	82.05 \pm 0.48	94.32 \pm 0.21	<u>79.00 \pm 3.39</u>	71.08 \pm 2.24	83.84 \pm 3.80
QS	99.25 \pm 0.47	87.86 \pm 0.72	88.78 \pm 1.86	91.95 \pm 0.58	81.28 \pm 0.54	94.28 \pm 0.40	73.75 \pm 4.15	75.00 \pm 0.00	77.38 \pm 5.19
Fisher	96.86 \pm 0.43	85.50 \pm 0.30	81.42 \pm 0.59	84.86 \pm 0.15	72.06 \pm 0.08	90.94 \pm 0.24	60.00 \pm 1.58	63.90 \pm 0.00	<u>90.50 \pm 0.00</u>
CIFE	74.70 \pm 0.00	85.30 \pm 0.00	55.40 \pm 0.00	87.60 \pm 0.00	68.40 \pm 0.00	82.70 \pm 0.00	50.00 \pm 0.00	69.40 \pm 0.00	52.40 \pm 0.00
ICAP	99.70 \pm 0.00	89.20 \pm 0.00	70.60 \pm 0.00	87.80 \pm 0.00	65.50 \pm 0.00	93.50 \pm 0.00	80.00 \pm 0.00	63.90 \pm 0.00	81.00 \pm 0.00
RFS	98.30 \pm 0.00	89.70 \pm 0.00	90.40 \pm 0.00	-	-	94.70 \pm 0.00	75.00 \pm 0.00	-	90.50 \pm 0.00
RCN	100.00 \pm 0.00	90.32 \pm 1.26	92.65 \pm 0.52	95.30 \pm 0.12	85.70 \pm 0.22	95.76 \pm 0.13	72.50 \pm 9.35	76.11 \pm 1.52	90.48 \pm 0.00
RCN flex	100.00 \pm 0.00	91.12 \pm 1.33	92.19 \pm 0.47	95.41 \pm 0.21	85.49 \pm 0.29	95.91 \pm 0.18	78.00 \pm 6.71	75.00 \pm 3.40	90.48 \pm 0.00
Learner: KNN									
All	100.00	87.85	88.14	96.91	84.96	97.37	92.50	69.44	76.19
NeuroFS	99.80 \pm 0.28	84.64 \pm 1.77	85.96 \pm 1.53	91.64 \pm 0.57	80.12 \pm 0.87	96.18 \pm 0.49	74.00 \pm 5.15	64.42 \pm 5.38	85.86 \pm 4.67
LassoNet	98.84 \pm 0.20	88.70 \pm 0.57	79.22 \pm 0.47	91.38 \pm 0.36	79.30 \pm 0.20	95.70 \pm 0.26	67.50 \pm 7.75	68.90 \pm 4.07	82.86 \pm 3.80
STG	99.94 \pm 0.12	87.86 \pm 0.39	83.16 \pm 3.42	87.16 \pm 0.64	77.65 \pm 0.48	95.14 \pm 0.45	75.00 \pm 5.24	58.90 \pm 7.52	81.00 \pm 0.00
QS	98.80 \pm 0.38	85.88 \pm 1.13	82.38 \pm 3.12	89.30 \pm 0.76	76.65 \pm 0.51	95.17 \pm 0.45	75.00 \pm 3.54	66.70 \pm 0.00	65.47 \pm 8.37
Fisher	95.80 \pm 0.00	81.10 \pm 0.00	74.10 \pm 0.00	80.20 \pm 0.00	63.70 \pm 0.00	88.80 \pm 0.00	70.00 \pm 0.00	50.00 \pm 0.00	85.70 \pm 0.00
CIFE	71.20 \pm 0.00	71.80 \pm 0.00	44.60 \pm 0.00	82.90 \pm 0.00	61.60 \pm 0.00	59.60 \pm 0.00	70.00 \pm 0.00	44.40 \pm 0.00	57.10 \pm 0.00
ICAP	98.60 \pm 0.00	82.70 \pm 0.00	59.00 \pm 0.00	83.40 \pm 0.00	59.30 \pm 0.00	94.00 \pm 0.00	65.00 \pm 0.00	61.10 \pm 0.00	66.70 \pm 0.00
RFS	97.20 \pm 0.00	90.30 \pm 0.00	87.20 \pm 0.00	-	-	95.40 \pm 0.00	85.00 \pm 0.00	-	90.50 \pm 0.00
RCN	99.93 \pm 0.16	86.43 \pm 0.93	88.21 \pm 0.46	94.48 \pm 0.20	82.01 \pm 0.20	96.65 \pm 0.20	73.00 \pm 7.37	58.89 \pm 4.12	87.62 \pm 2.61
RCN flex	99.79 \pm 0.31	86.40 \pm 1.14	87.12 \pm 0.69	94.62 \pm 0.24	82.10 \pm 0.56	96.48 \pm 0.39	76.50 \pm 2.24	62.22 \pm 6.09	89.52 \pm 2.13
Learner: SVM									
All	100.00	95.05	96.03	97.92	88.30	97.58	77.50	72.22	80.95
NeuroFS	98.78 \pm 0.29	91.46 \pm 0.72	92.62 \pm 0.40	95.30 \pm 0.41	83.78 \pm 0.64	96.78 \pm 0.17	76.50 \pm 2.55	80.54 \pm 4.96	90.50 \pm 0.00
LassoNet	97.16 \pm 1.06	93.74 \pm 0.39	84.90 \pm 0.22	94.46 \pm 0.21	82.58 \pm 0.10	95.94 \pm 0.15	71.00 \pm 2.00	74.46 \pm 4.78	88.58 \pm 2.35
STG	99.32 \pm 0.40	91.22 \pm 1.23	85.82 \pm 2.83	93.20 \pm 0.62	82.36 \pm 0.52	96.62 \pm 0.34	71.00 \pm 2.55	70.00 \pm 2.08	84.78 \pm 3.55
QS	96.52 \pm 1.53	91.96 \pm 1.04	89.78 \pm 1.80	93.62 \pm 0.49	80.82 \pm 0.51	95.52 \pm 0.27	74.38 \pm 4.80	72.20 \pm 2.80	76.20 \pm 7.53
Fisher	74.00 \pm 0.00	79.80 \pm 0.00	67.40 \pm 0.00	81.90 \pm 0.00	67.80 \pm 0.00	91.00 \pm 0.00	67.50 \pm 0.00	63.90 \pm 0.00	90.50 \pm 0.00
CIFE	59.40 \pm 0.00	84.20 \pm 0.00	59.80 \pm 0.00	89.30 \pm 0.00	66.90 \pm 0.00	61.30 \pm 0.00	52.50 \pm 0.00	58.30 \pm 0.00	47.60 \pm 0.00
ICAP	99.30 \pm 0.00	88.70 \pm 0.00	75.10 \pm 0.00	89.00 \pm 0.00	59.50 \pm 0.00	95.20 \pm 0.00	70.00 \pm 0.00	72.20 \pm 0.00	57.10 \pm 0.00
RFS	95.80 \pm 0.00	94.00 \pm 0.00	91.50 \pm 0.00	-	-	95.80 \pm 0.00	77.50 \pm 0.00	-	90.50 \pm 0.00
RigL	97.86 \pm 1.32	91.82 \pm 0.30	89.58 \pm 1.24	93.94 \pm 0.63	81.92 \pm 0.87	96.04 \pm 0.58	77.00 \pm 3.32	70.54 \pm 4.16	79.06 \pm 7.11
RCN	99.58 \pm 0.29	93.74 \pm 0.62	93.41 \pm 0.25	96.69 \pm 0.19	85.95 \pm 0.22	96.83 \pm 0.17	72.50 \pm 5.59	73.33 \pm 1.52	90.48 \pm 0.00
RCN flex	99.51 \pm 0.19	93.65 \pm 0.36	93.46 \pm 0.19	96.79 \pm 0.11	85.84 \pm 0.36	97.06 \pm 0.23	76.00 \pm 6.75	74.44 \pm 2.32	89.52 \pm 2.13